Benchmarking aerodynamic prediction of unsteady rotor aerodynamics of active flaps on wind turbine blades using ranging fidelity tools

2016 J. Phys.: Conf. Ser. 753 022027

(http://iopscience.iop.org/1742-6596/753/2/022027)

Benchmarking aerodynamic prediction of unsteady rotor aerodynamics of active flaps on wind turbine blades using ranging fidelity tools

Thanasis Barlas[1], Eva Jost[2], Georg Pirrung[1], Theofanis Tsiantas[3], Vasilis Riziotis[3], Sachin T. Navalkar[4], Thorsten Lutz[2] and Jan-Willem van Wingerden[4]

1 Technical University of Denmark, Department of Wind Energy, Aerodynamic Design & Loads and Control, DTU Risø Campus, Fredriksborgvej 399, 4000 Roskilde
2 Institute of Aerodynamics and Gas Dynamics, University of Stuttgart, Pfaffenwaldring 21, 70569 Stuttgart Germany
3 National Technical University of Athens, School of Mechanical Engineering, Section of Fluids, Heroon Polytechniou 9, 15780 Zografou, Athens, Greece
4 Delft University of Technology, Delft Center for Systems and Control, Faculty of Mechanical Engineering, 2628 CD Delft, the Netherlands

E-mail: tkba@dtu.dk

Abstract.
Simulations of a stiff rotor configuration of the DTU 10MW Reference Wind Turbine are performed in order to assess the impact of prescribed flap motion on the aerodynamic loads on a blade sectional and rotor integral level. Results of the engineering models used by DTU (HAWC2), TUDelft (Bladed) and NTUA (hGAST) are compared to the CFD predictions of USTUTT-IAG (FLOWer). Results show fairly good comparison in terms of axial loading, while alignment of tangential and drag-related forces across the numerical codes needs to be improved, together with unsteady corrections associated with rotor wake dynamics. The use of a new wake model in HAWC2 shows considerable accuracy improvements.

1. Introduction

The size of wind turbines has been increasing rapidly over the past years. Rotors of more than 160m in diameter are already commercially available. Focusing on lowering the cost per kWh, new trends and technological improvements have been primary targets of research and development. One main focus is on developing new technologies, which are, amongst other, capable of considerably reducing fatigue loads on wind turbines. New concepts for dynamic load reduction are focusing on a much faster and localized load control, compared to existing individual blade pitch control, by utilizing active aerodynamic control devices distributed along the blade span [1]. Such concepts are generally referred to as smart rotor control, a term used in rotorcraft research, and investigated for wind turbine applications over the past years in terms of conceptual and aeroelastic analysis, small scale wind tunnel experiments, and recently field testing [2, 3, 4, 5, 6]. For a review of the state-of-the-art in the topic, the reader is referred to [1]. So far, results from numerical and experimental analysis mostly focusing on trailing edge

flaps have shown a considerable potential in fatigue load reduction [7, 8]. Existing work has provided aeroelastic tools with the capability of simulating active flap configurations, however the accuracy of such tools has not been verified in detail compared to higher fidelity ones.
The objective in focus is the investigation of the purely aerodynamic effect of trailing edge flaps on the resulting blade loads and power of the wind turbine, as they constitute a potential future means of load alleviation [5, 1]. In this process, the current numerical tools for wind turbine analysis are extended to incorporate the new actuators, and are validated at representative operating conditions against Computational Fluid Dynamics (CFD) simulations, which act as a high fidelity benchmark.

2. Model and operating cases

The turbine model used is the DTU 10 MW turbine, which is a reference turbine with a rotor diameter of 178.3 m, described fully in [9]. Simulated cases concern a uniform constant wind input and constant rotor speed and blade pitch angle. The prescribed collective flap input consists of a sinusoidal signal with max/min flap amplitude and frequency relevant multiples of the rotor frequency (1p, 3p, and 6p) at representative operating points. The list of simulated cases is shown in Table 1. All cases utilise a stiff structure configuration, no blades precone, no rotor tilt and the prescribed control inputs.

Table 1. Operating parameters of simulated cases.

Case	11.4m/s - $1p_{sine}$	11.4m/s - $3p_{sine}$	11.4m/s - $6p_{sine}$	19.0m/s - $6p_{sine}$
wind speed [m/s]	11.4	11.4	11.4	11.4
rotor speed [rpm]	9.6	9.6	9.6	9.6
pitch angle [deg]	0	0	0	16.432
flap [deg]	$\pm 10 \cdot sin(1 \cdot p \cdot t)$	$\pm 10 \cdot sin(3 \cdot p \cdot t)$	$\pm 10 \cdot sin(6 \cdot p \cdot t)$	$\pm 10 \cdot sin(6 \cdot p \cdot t)$

The simulated flap configuration comprises of a 10% chord-wise length flap, covering 10% of the blade length , which is chosen based on prior studies [8], and the configuration for the INNWIND.EU project (conservative flap system extent). The flap system parameters are shown in Table 2.

Table 2. Parameters of simulated flap configuration.

Flap configuration	
Chordwise extension	10%
Deflection angle limits	±10deg
Spanwise length	8.9m (10% of blade length)
Spanwise location	71.32m-62.40m (from rotor center)
Airfoil	FFA-W3-241
Max ΔC_L	±0.4

Engineering tools based on the Blade Element Momentum (BEM) method with various corrections are utilized and compared to CFD simulations. The utilized tools and corresponding research partners are : FLOWer(USTUTT-IAG), HAWC2(DTU), hGAST(NTUA), and Bladed (TUDelft). The CFD code FLOWer was originally developed by the German Aerospace Center (DLR) [10, 11] and is a block-structured compressible (U)RANS solver. The aeroelastic code

HAWC2 [12] is a BEM-based tool using a multi-body approach. The unsteady aerodynamics associated with the active flaps is accounted for by using the ATEFlap dynamic stall model in HAWC2 [13]. The variation of steady lift, drag, and moment coefficients introduced by the flap deflection in based on 2D CFD simulations performed with the code Ellipsys2D [14]. The actuator dynamics are implemented as a linear servo model in HAWC2, for a first order system with a time constant of 0.1s, as representative for a Controllable Rubber Trailing Edge Flap (CRTEF) actuator [5]. The near wake model [15] accounts for the dynamic effects of the trailed vorticity close to the blade. The aeroelastic code hGAST [16] is a BEM-based tool using a multi-body approach. The unsteady aerodynamics associated with the TE active shape variations is accounted for by using the inviscid aerodynmamics model FOILFS enhanced with the ONERA model to account for dynamic stall conditions. Input steady-state lift, drag, and moment characteristics for the various airfoil deflected shapes have been simulated using NTUA's in-house viscous-inviscid interaction code FOIL2W [17]. The flap actuator dynamics are modelled as in HAWC2. GH Bladed^{TM} is a commercial software validated with experimental data and used for evaluating the performance of turbines with trailing edge flap actuators [18]. The software uses a multi-body structural approach with the rotor aerodynamics modelled using BEM, with further corrections for tip effects and three-dimensional flow. The quasi-steady aerodynamic polars used are the same as in the case of hGAST.

3. Results

The presented simulation results consist of time series and radial distribution of sectional loads (out-of-plane and in-plane forces) at the 75% radial section (flap mid-span) and the integral rotor response (thrust and power), shown for one revolution. For the case of 11.4 m/s with a 1p flap excitation, the rotor thrust and power are shown in Fig. 1 and Fig. 2. The sectional axial (out-of-plane) and tangential (in-plane) force radial distributions are shown for the time instance when the flap is at maximum positive position (Fig. 3 and 4), and when the flap is at maximum negative position (Fig. 5 and 6).

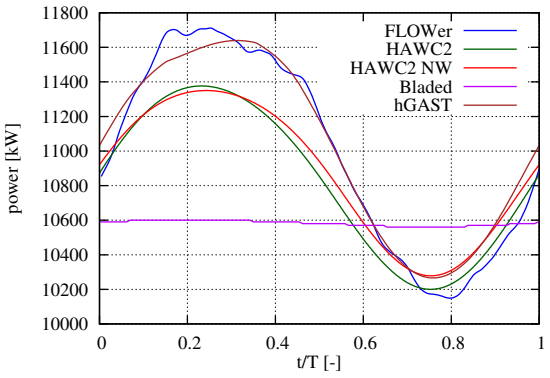

Figure 1. Comparison of rotor power time series over one revolution (11.4m/s - 1p flap).

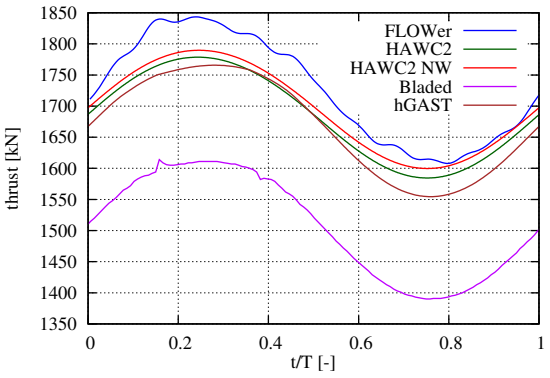

Figure 2. Comparison of rotor thrust time series over one revolution (11.4m/s - 1p flap).

It is seen that the predictions of the thrust force variation in time due to the flap action are comparing well, but power is overpredicted by CFD compared to the engineering models due to a higher prediction of tangential force variation resulting from the drag forces. As the CFD simulations have been conducted under fully turbulent conditions, a higher drag is expected with regard to the provided polars. In terms of radial distribution, the axial force comparison is

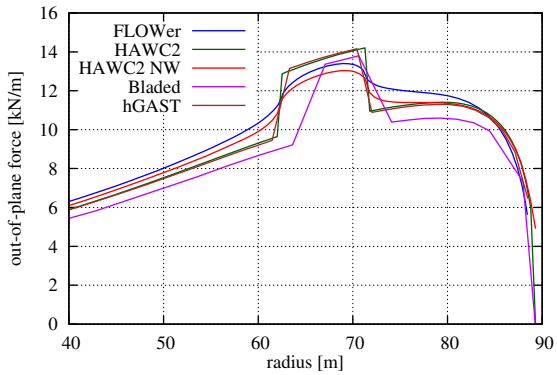

Figure 3. Comparison of radial distribution of axial aerodynamic forces at the extreme positive flap angle position (11.4m/s - 1p flap).

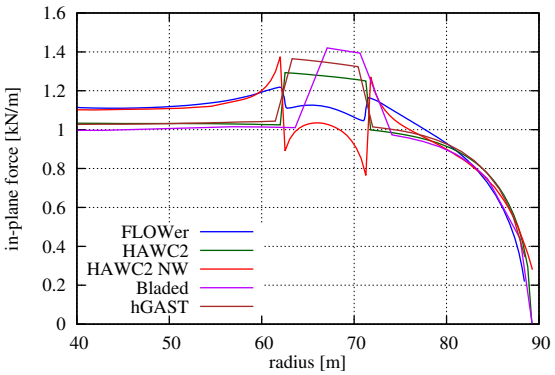

Figure 4. Comparison of radial distribution of tangential aerodynamic forces at the extreme positive flap angle position (11.4m/s - 1p flap).

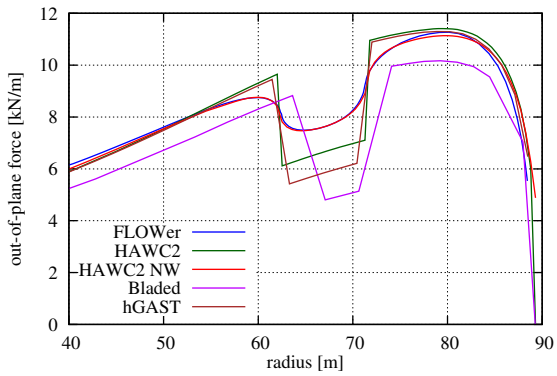

Figure 5. Comparison of radial distribution of axial aerodynamic forces at the extreme negative flap angle position (11.4m/s - 1p flap).

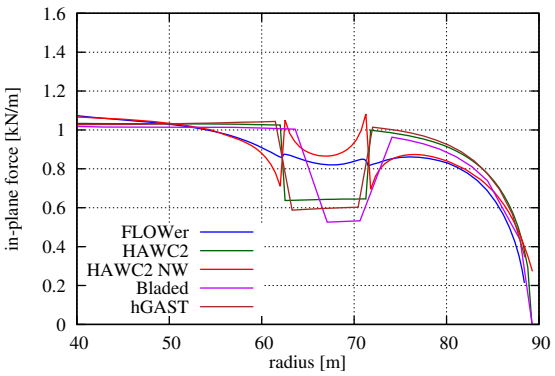

Figure 6. Comparison of radial distribution of tangential aerodynamic forces at the extreme negative flap angle position (11.4m/s - 1p flap).

fair, with the expected smoothing of distribution around the flap region predicted by CFD, and only captured by the near wake implementation of HAWC2. The tangential force distribution prediction of the engineering models is quite different compared to the CFD results, with the local increase/decrease due to the flap action being more evident, predicting a force increase all over the flap region. Only the near wake HAWC2 implementation is able to capture the specific force distribution closer to CFD. Bladed results show a discrepancy in predicting the correct shape and amplitude of the tangential force response, thus resulting in underestiation of thrust and power variations.

For the case of 11.4 m/s with a 6p flap excitation, the rotor thrust and power are shown in Fig. 7 and Fig. 8. The sectional axial (out-of-plane) and tangential (in-plane) force radial distributions are shown for the time instance when the flap is at maximum positive position (Fig. 9 and 10), and when the flap is at maximum negative position (Fig. 11 and 12).

In this case, the thrust force variations in time due to the flap action are slightly overpredicted

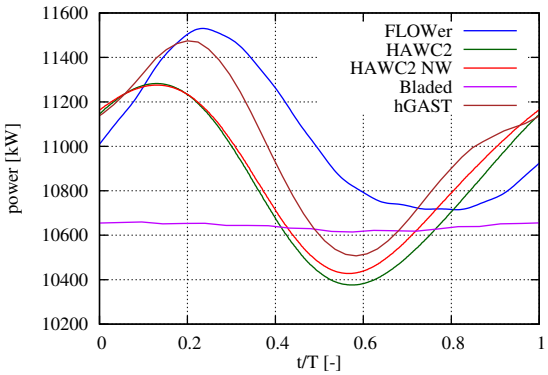

Figure 7. Comparison of rotor power time series over one revolution (11.4m/s - 6p flap).

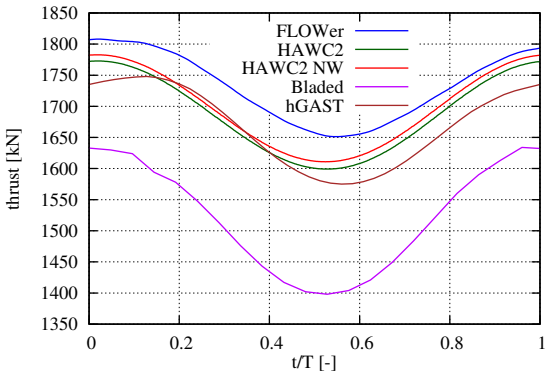

Figure 8. Comparison of rotor thrust time series over one revolution (11.4m/s - 6p flap).

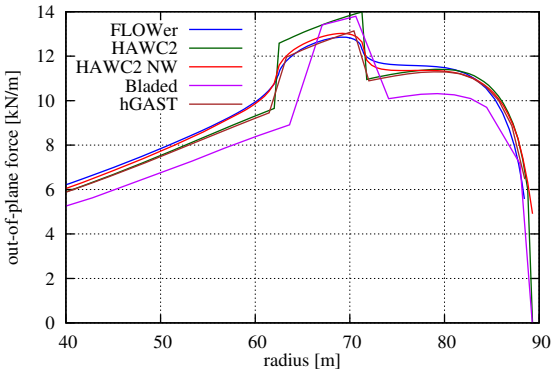

Figure 9. Comparison of radial distribution of axial aerodynamic forces at the extreme positive flap angle position (11.4m/s - 6p flap).

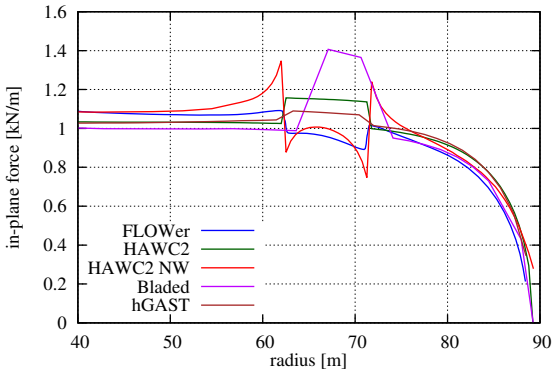

Figure 10. Comparison of radial distribution of tangential aerodynamic forces at the extreme positive flap angle position (11.4m/s - 6p flap).

in the engineering models, and the CFD code predicts a larger phase in the power response. In terms of radial distribution, both the axial and tangential force comparisons show an overprediction of the variation by the engineering models, as compared to the smooth distribution around the flap region predicted by CFD and the near wake model with HAWC2.

For the case of 19 m/s with a 6p flap excitation, the rotor thrust and power are shown in Fig. 13 and Fig. 14. The sectional axial (out-of-plane) and tangential (in-plane) force radial distributions are shown for the time instance when the flap is at maximum positive position (Fig. 15 and 16), and when the flap is at maximum negative position (Fig. 17 and 18).

In this case, the thrust force and power variations in time due to the flap action compare well between the engineering models and CFD. In terms of radial distribution, both the axial and tangential force comparisons show an overprediction of the variation by the engineering models, as compared to the smooth distribution around the flap region predicted by CFD and the near wake model with HAWC2.

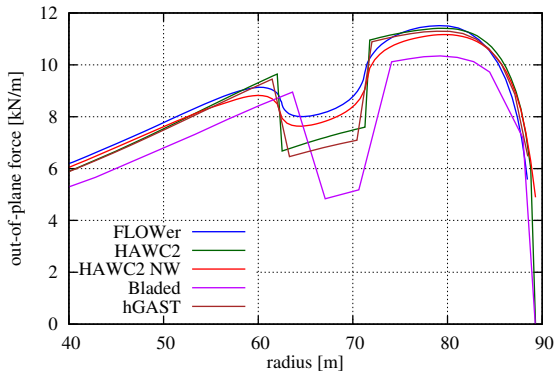

Figure 11. Comparison of radial distribution of axial aerodynamic forces at the extreme negative flap angle position (11.4m/s - 6p flap).

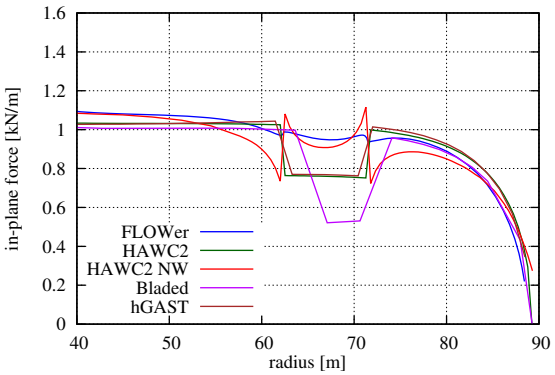

Figure 12. Comparison of radial distribution of tangential aerodynamic forces at the extreme negative flap angle position (11.4m/s - 6p flap).

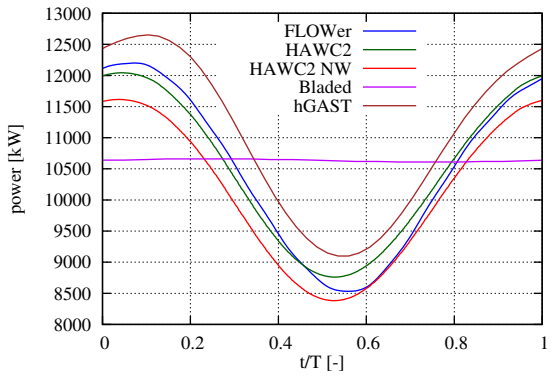

Figure 13. Comparison of rotor power time series over one revolution (19m/s - 6p flap).

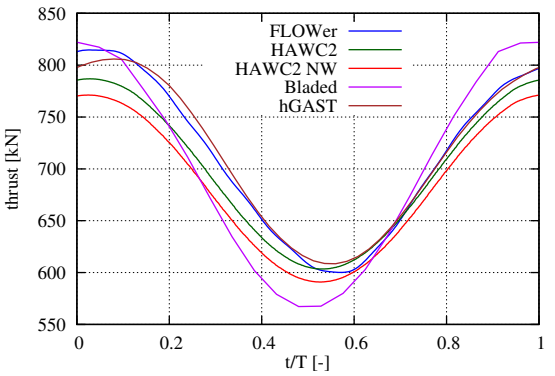

Figure 14. Comparison of rotor thrust time series over one revolution (19m/s - 6p flap).

4. Conclusion

Overall, the prediction of the variation of the flap mid-span sectional axial force compares fairly well between CFD and the engineering models. The flap mid-span tangential force is largely over-predicted in the engineering models, while it is captured very accurately when using the near wake model in HAWC2.

Compared to the engineering codes, CFD overpredicts power variation, while it compares better at higher flap frequencies. Among the engineering models, it is seen that the prediction of the tangential force variation of Bladed is the highest, however it remains within reasonable bounds. The response of the engineering models comes closer to the CFD predictions at higher wind speeds, which is also the region where trailing edge flaps are expected to be used to the greatest extent. For more advanced applications, closer attention is required to be devoted to correlating other aerodynamic phenomena. Further insight into 3D aerodynamic effects are expected in future research investigations, and detailed evaluation of engineering code predictions in a full aero-servo-elastic environment.

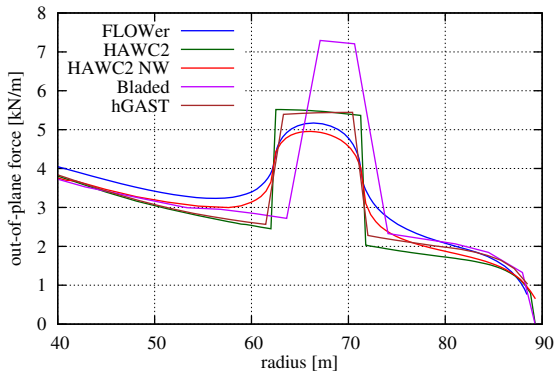

Figure 15. Comparison of radial distribution of axial aerodynamic forces at the extreme positive flap angle position (19m/s - 6p flap).

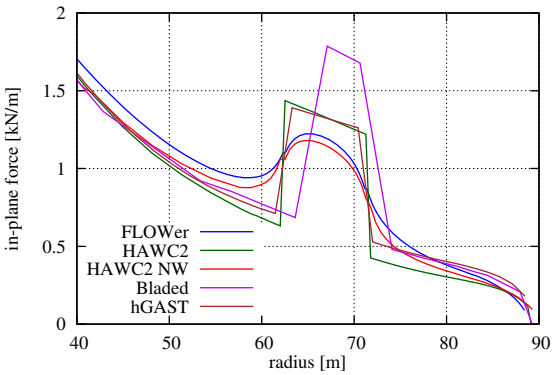

Figure 16. Comparison of radial distribution of tangential aerodynamic forces at the extreme positive flap angle position (19m/s - 6p flap).

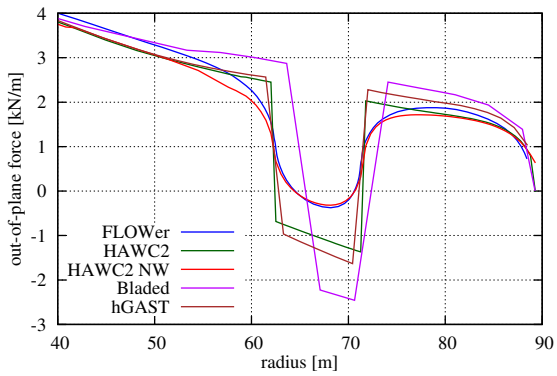

Figure 17. Comparison of radial distribution of axial aerodynamic forces at the extreme negative flap angle position (19m/s - 6p flap).

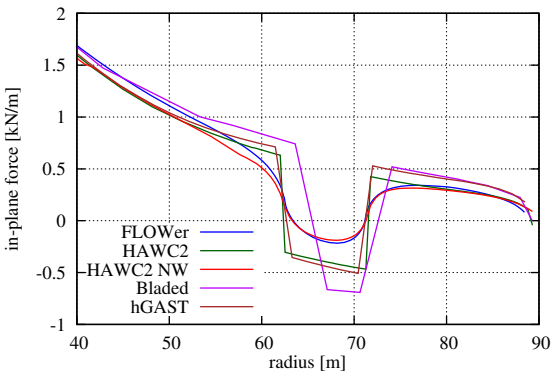

Figure 18. Comparison of radial distribution of tangential aerodynamic forces at the extreme negative flap angle position (19m/s - 6p flap).

Acknowledgments

The research leading to these results has received funding from the European Community's Seventh Framework Programme under grant agreement No. 308974 (INNWIND.EU)

References

[1] Barlas T. K. and van Kuik G. A. M. Review of state of the art in smart rotor control research for wind turbines *Progress in Aerospace Sciences - 2010* **46** 1 pp 1-27 2010

[2] Van Wingerden, J., Hulskamp, A., Barlas, T., Houtzager, I., Bersee, H., van Kuik, G., and Verhaegen, M., *Two-degree-of-freedom active vibration control of a prototyped 'smart' rotor*. Control Systems Technology, IEEE Transactions on, 19(2), 284-296, 2011.

[3] Madsen H. A., Andersen P. B., Andersen T., Bak C. and Buhl T., *The potentials of the controllable rubber trailing edge flap (CRTEF)*. Proceedings of EWEC 2010, 20-23 April 2010, Warsaw, Poland

[4] Barlas, T. K. and Madsen, H. A., *Influence of Actuator Dynamics on the Load Reduction Poetntial of Wind Turbines with Distributed Controllable Rubber Trailing edge Flaps (CRTEF)*. Proceedings

of ICAST2011: 22nd International Conference on Adaptive Structures and Technologies, October 10-12, 2011, Corfu, Greece.

[5] Madsen H. A. et al. Towards an industrial manufactured morphing trailing edge flap system for wind turbines *Proceedings of EWEC 2014, Barcelona, Spain* 2014

[6] Castaignet, D., Barlas, T., Buhl, T., Poulsen, N. K., Wedel-Heinen, J. J., Olesen, N. A., Bak, C., and Kim, T., *Full-scale test of trailing edge flaps on a Vestas V27 wind turbine: active load reduction and system identification*. Wind Energy, 17(4), 549-564, 2014.

[7] Barlas, T., *Active aerodynamic load control on wind turbine blades: Aeroservoelastic modelling and wind tunnel experiments*, PhD thesis, TUDelft, 2011.

[8] Bergami, L., *Adaptive Trailing Edge Flaps for Active Load Alleviation in a Smart Rotor Configuration*, PhD thesis, DTU Wind Energy, 2013.

[9] Bak C. et al Description of the DTU 10 MW Reference Wind Turbine *Technical report, DTU Vindenergi-I-0092* 2013

[10] Meister K. Krämer E. and Lutz T. Development of a process chain for detailed wake simulation of horizontal axis wind turbines *EUROMECH 2009 Madrid* 2009

[11] Schulz C. et al Evaluation and Control of Wind Turbines under Different Operation Conditions by means of CFD *High Performance Computing in Science and Engineering, Springer International Publishing* 2015

[12] Larsen T. J. et al. How 2 Hawc2, the user's manual *Technical report, Risø-R-1597(ver. 4-4)(EN)* 2013

[13] Bergami L. and Gaunaa M. ATEFlap Aerodynamic Model, a dynamic stall model including the effects of trailing edge flap deflection *Technical report, Risø-R-1792(EN)* 2012

[14] Sørensen N. N. General purpose flow solver applied to flow over hills *Technical Report Risø-R-827(EN)* 1995.

[15] Pirrung G. R. Madsen H. A. Kim T. and Heinz J. Improvement of a near wake model for trailing vorticity *Wind Energy* DOI:10.1002/we.1969 2016

[16] Manolas D. I. Riziotis V. A. and Voutsinas S. G. Assessing the importance of geometric non-linear effects in the prediction of wind turbine blade loads *Computational and Nonlinear Dynamics Journal* **10** 041008 2015

[17] Riziotis V. A. and Voutsinas S. G. Dynamic stall modeling on airfoils based on strong viscous-inviscid interaction coupling *J. Numerical Methods in Fluids* **56** pp 185-208 2008

[18] Lackner A. L. and van Kuik G. A. M. A Comparison of Wind Turbine Smart Rotor Control Approaches using Trailing Edge Flaps and Individual Pitch Control *Wind Energy* **13** pp 117-134 2010